Acta Crystallographica Section D
Biological Crystallography
ISSN 0907-4449

Structures of the deoxy and CO forms of haemoglobin from *Dasyatis akajei*, a cartilaginous fish

Khoon Tee Chong,[a] Gentaro Miyazaki,[a] Hideki Morimoto,[a]* Yutaka Oda[b] and Sam-Yong Park[c]

[a]Division of Biophysical Engineering, Graduate School of Engineering Science, Osaka University, Toyonaka, Osaka 560-8531, Japan, [b]Department of Biology, Graduate School of Science, Osaka University, Toyonaka, Osaka 560-0043, Japan, and [c]The Institute of Physical and Chemical Research (RIKEN), RIKEN Harima Institute, Mikazuki-cho, Sayo, Hyogo 679-5143, Japan

Correspondence e-mail: morimoto@bpe.es.osaka-u.ac.jp

Received 25 March 1999
Accepted 27 April 1999

PDB References: deoxy form of haemoglobin, 1cg5; CO form of haemoglobin, 1cg8.

The three-dimensional structures of the deoxy- and carbonmonoxyhaemoglobin (Hb) from *Dasyatis akajei*, a stingray, have been determined at 1.6 and 1.9 Å resolution, respectively. This is one of the most distantly related vertebrate Hbs to human HbA. Both structures resemble the respective forms of HbA, indicating that the $\alpha_2\beta_2$-type tetramer and the mode of the quaternary structure change are common to Hbs of jawed vertebrates. Larger deviations between *D. akajei* Hb and human HbA are observed in various parts of the molecule, even in the *E* and *F* helices. Significant mutations and/or conformational changes are also observed around the haems, in the C-terminal region of the β subunit, in the $\alpha_1\beta_2$ interface and in the organic phosphate-binding site of HbA. Despite these structural differences, the oxygen affinity, haem–haem interaction, Bohr effect and organic phosphate effect of *D. akajei* Hb are all only moderately reduced. Compared with human HbA, the overall r.m.s. deviation of main-chain atoms in the helical regions of bony fish Hbs is smaller than that of *D. akajei* Hb.

1. Introduction

Since the three-dimensional structures of human and horse haemoglobins (Hbs) were determined, various properties of other vertebrate Hbs have been studied on the basis of these structures, assuming that tertiary and quaternary structures of Hbs of jawed vertebrates (with the exception of Agnatha) are all essentially the same (Perutz, 1983). X-ray crystallographic and molecular-evolutional studies have shown that the tertiary structure of globins is also conserved in invertebrates and is designated the globin fold (Lesk & Chothia, 1980; Bashfold *et al.*, 1987). X-ray crystallography has shown that there are two quaternary structures, one liganded (Shaanan, 1983) and the other unliganded (Fermi *et al.*, 1984). Both are assumed to be common among jawed vertebrate Hbs, which adopt one or the other structure depending on the presence of ligand at the haems (Baldwin & Chothia, 1979). The higher occurrence of invariant residues at the $\alpha_1\beta_2$ and $\alpha_1\beta_1$ interfaces compared with other surface regions of the subunits supports this assumption. The X-ray structures of the carbonmonoxy-Hb and deoxy-Hb of *Pagothenia bernacchii*, a bony fish, provided the first structural evidence that the allosteric change in human Hb is common to vertebrates from mammals to bony fish (Camardella *et al.*, 1992; Ito *et al.*, 1995). X-ray structures for the CO and deoxy forms of a trout (*Oncorhyncus mykiss*) Hb (Tame *et al.*, 1996), the CO form of another bony fish (*Leiostomus xanthurus*) Hb (Mylvaganam *et al.*, 1996) and the oxy form of bar-headed goose Hb (Zhang *et al.*, 1996) are also available. All these structures adopt one or other of the previously described forms of human Hb. Here, we describe

the liganded and unliganded structures of Hb from a cartilaginous fish (*Dasyatis akajei*). This Hb is more distantly related to human Hb than any previously structurally characterized Hb. Although the overall structures of *D. akajei* Hb and human HbA are very similar, significant structural differences were found in the functionally important regions. We discuss the properties of the protein in relation to its structure and compare it with Hb from bony fish.

2. Materials and methods

2.1. Haemoglobin

Live fish (*D. akajei*) were obtained from Taniume, a fish dealer of the port of Minoshima in the Wakayama Prefecture, Japan. Blood was collected from the vein near the heart using a heparinized syringe. The erythrocytes were washed three times in cold saline and lysed by the addition of three volumes of distilled water. The nucleic acid aggregate and cell debris were removed by centrifugation at 12000*g* for 20 min. The supernatant was then applied to Sephadex G-25 equilibrated with 0.01 *M* tris(hydroxymethyl)aminomethane (Tris) buffer at pH 7.2 and loaded onto an ion-exchange column (Whatman DE-32) equilibrated with the same buffer. It was eluted with a linear salt gradient from 0.02 to 0.5 *M*. The main band was collected, concentrated and stored as the CO form at 193 K. The electrophoretic patterns of *D. akajei* haemolysate show the presence of a single major haemoglobin and two minor components (about 5% in total). The procedure described here removed these minor components. These minor components might be modified forms of the main component, since we detected only one cDNA sequence, as described below.

2.2. cDNA sequence analysis

The α and β chain of *D. akajei* Hb were prepared by the methods of Suzuki & Nishikawa (1996). The N-terminal amino-acid sequences of the α and β chains were determined with an automated protein sequencer (Model 476A, Applied BioSystems). mRNA was isolated from the *D. akajei* erythrocytes with a FastTrack mRNA Isolation Kit (Invitrogen). The single-stranded cDNA was synthesized with a Ready-To-Go T-Primed First-Strand Kit (Pharmacia) and purified using a QIAquick PCR purification Kit (QIAGEN). The nucleotide sequences of the cDNA from both the α and β chains of *D. akajei* Hb were determined using the methods of Suzuki *et al.* (1996). Three cDNAs from the α chain and four cDNAs from the β chain were analyzed and an identical result was obtained for each.

The nucleotide-sequence data reported in this paper will appear in the DDBJ/EMBL/Genbank nucleotide sequence databases with the accession numbers AB023722 (α chain) AB023723 (β chain).

2.3. Oxygen equilibrium measurement

Oxygen equilibrium curves were measured as described by Imai *et al.* (1970). Measurements were carried out on purified *D. akajei* Hb at 298 K in 50 m*M* 2-[bis(2-hydroxymethyl)amino]-2-hydroxymethyl-1,3-propanediol (bis–Tris) or Tris buffer with 100 m*M* chloride. In order to reduce methaemoglobin levels, catalase and superoxide dismutase were added to Hb samples (Lynch *et al.*, 1976; Winterbourn *et al.*, 1976). Deoxygenation curves were used to determine p_{50} (the oxygen partial pressure necessary to attain 50% saturation of Hb with oxygen) and the Hill coefficient n (the maximum slope of Hill plots of oxygen equilibrium curves). 2 m*M* ATP was used as an organic phosphate effector.

Table 1
Crystallographic data and refinement for *D. akajei* Hb.

Figures in parentheses refer to the highest resolution shell.

	Deoxy form	CO form
Crystal data		
Space group	$P3_112$	$C222_1$
Unit-cell parameters (Å, °)	$a = b = 77.76$, $c = 99.31$; $\alpha = \beta = 90$, $\gamma = 120$	$a = 57.36$, $b = 99.69$, $c = 107.55$; $\alpha = \beta = \gamma = 90$
Resolution range (Å)	100–1.6 (1.66–1.60)	100–1.9 (1.97–1.90)
Observed reflections	209235 (16933)	169395 (8574)
Independent reflections	42219 (3544)	23946 (2163)
Completeness (%)	92.7 (78.1)	95.9 (86.8)
R_{merge}† (%)	6.8 (26.4)	4.9 (23.7)
Refinement parameters		
Asymmetric unit	$\alpha\beta$ dimer	$\alpha\beta$ dimer
Resolution (Å)	8.0–1.6	6.0–1.9
Reflections with $F > 2\sigma$	41888	22945
R_{free} ‡(%)	23.2	25.2
R_{cryst} §(%)	19.1	19.7
Protein atoms	272	2272
CO, haem atoms	86	90
Water molecules	151	98
Average B factor (Å^2)		
Main-chain atoms	2.7	28.4
Side-chain atoms	17.1	33.9
COs, haems	15.3	27.2
All protein atoms	15.0	31.2
Waters	28.3	42.3
Deviations from ideality		
Bonds (Å)	0.008	0.007
Angles (°)	1.3	1.2
Dihedrals (°)	19.3	19.3
Improper dihedrals (°)	1.2	1.2
Ramachandran plot (%)		
Most-favoured regions	93.5	94.3
Additionally allowed regions	6.1	5.4
Generously allowed regions	0.4	0.4
Disallowed regions	0.0	0.0
Isotropic thermal factor restraints (r.m.s., σ)		
Main-chain bond	1.25, 1.50	2.23, 1.50
Main-chain angle	1.84, 2.00	3.37, 2.00
Side-chain bond	3.06, 2.00	4.10, 2.00
Side-chain angle	4.73, 2.50	6.37, 2.50

† $R_{merge} = \sum_h \sum_i |I(h,i) - \langle I(h)\rangle| / \sum_h \sum_i |I(h,i)|$, where $I(h,i)$ is the intensity value of the ith measurement of h and $\langle I(h)\rangle$ is the corresponding mean value of $I(h,i)$ for all i measurements; the summation is over the reflections with $I/\sigma(I) > 1.0$. ‡ R_{free} is the R factor calculated for 5% of reflections which were randomly selected and were excluded from the *X-PLOR* refinement. § $R_{cryst} = \sum ||F_o| - |F_c|| / \sum |F_o|$, where F_o is the observed structure factor and F_c is that calculated from the model.

2.4. Crystal growth and X-ray crystal structure determination

Both deoxy and CO-liganded crystals were grown at room temperature by batch crystallization under an atmosphere of

nitrogen and carbon monoxide, respectively. The tubes were sealed with well fitting rubber stoppers. Ammonium sulfate was used as the precipitant for crystallization of both the deoxy and CO forms. Deoxy crystals were obtained between 1.8 and 2.0 *M* at pH 6.5 and CO crystals were obtained between 2.1 and 2.3 *M* at the same pH using solution *C* described by Perutz (1968). The haemoglobin concentration for both deoxy- and CO-form crystallization was about 2%.

The deoxy-Hb data set was collected at the Photon Factory, Tsukuba, Japan using the Weissenberg camera (Sakabe, 1983). The HbCO data set was collected on an R-AXIS IIC imaging-plate system mounted on a Rigaku RU200 rotating-anode generator at the Protein Research Center, Osaka University. The data were processed with *DENZO* and scaled with *SCALEPACK* (Otwinowski & Minor, 1997).

Both structures were solved by the molecular-replacement method (Rossmann & Blow, 1962). The rotation-function and translation searches were carried out using *X-PLOR* (Brünger, 1992). Data between 10.0 and 5.0 Å were used in both cases. The initial model for an $\alpha\beta$ dimer of the deoxy form was constructed from human deoxy-Hb by substituting appropriate side chains and deleting four residues in the *D* helix and one residue in the *FG* corner of the β-chain. Initial model refinement was carried out by simulated annealing

Table 2
Oxygen equilibrium characteristics of *D. akajei* Hb.

Experimental conditions are 298 K, 60 m*M* (haem) Hb and 100 m*M* chloride.

pH	p_{50}† (Pa)	n‡
6.5 (−)	3720 ± 110 (4)	1.9
6.5 (+)	8190 ± 650 (2)	1.3
7.4 (−)	1570 ± 90 (2)	2.1
7.4 (+)	2490 ± 50 (3)	2.1
8.5 (−)	560 ± 30 (4)	2.1
8.5 (+)	570 ± 40 (3)	2.0

† p_{50}, oxygen partial pressure necessary to attain 50% saturation of Hb with oxygen without (−) and with (+) 2 m*M* ATP. The number of the determinations are given in parentheses and errors (the standard deviations) are calculated from them. ‡ n, Hill coefficient (the maximum slope of Hill plots of oxygen equilibrium curves).

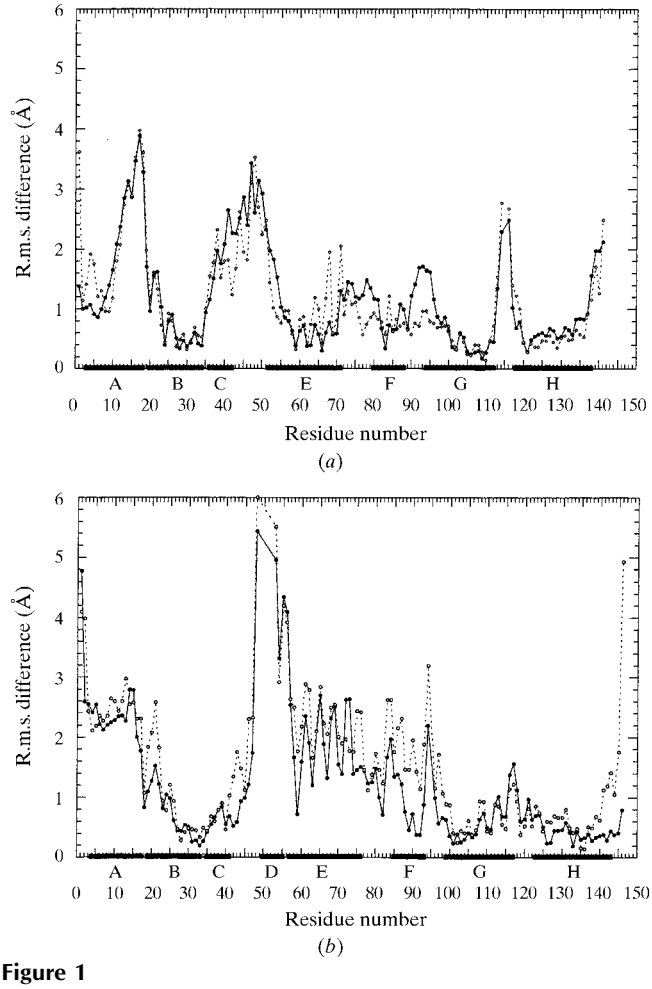

Figure 1
The r.m.s. deviations of main-chain atoms between *D. akajei* Hb and human HbA against residue number along the chain in the BGH frame. (*a*) α subunit, (*b*) β subunit. Solid line with closed circles, CO form; broken line with open circles, deoxy form. The residue numbers are those of human HbA and therefore no points are marked at the deleted position of *D. akajei* Hb. The BGH core residues used for the superposition are the main-chain atoms B5–B15, G4–G18, H3–H17 for both the α and β subunits.

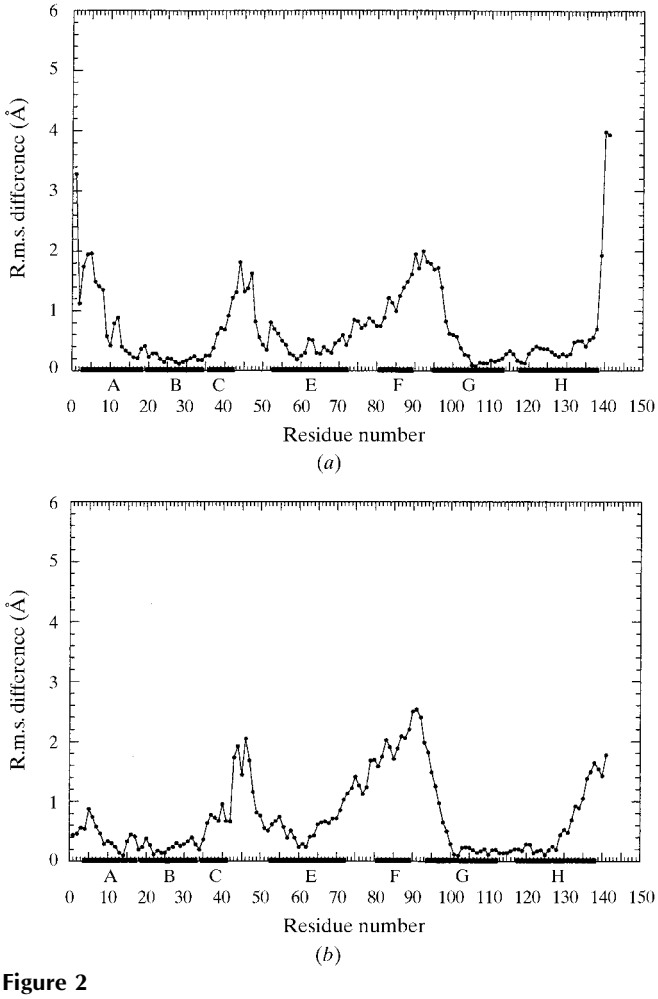

Figure 2
The r.m.s. deviations of main-chain atoms in the $\alpha_1\beta_1$ contact of CO *D. akajei* Hb compared with those of the deoxy form against residue number along the chain after superposition of the BGH core residues presented in the legend of Fig. 1. (*a*) α_1 subunit, (*b*) β_1 subunit.

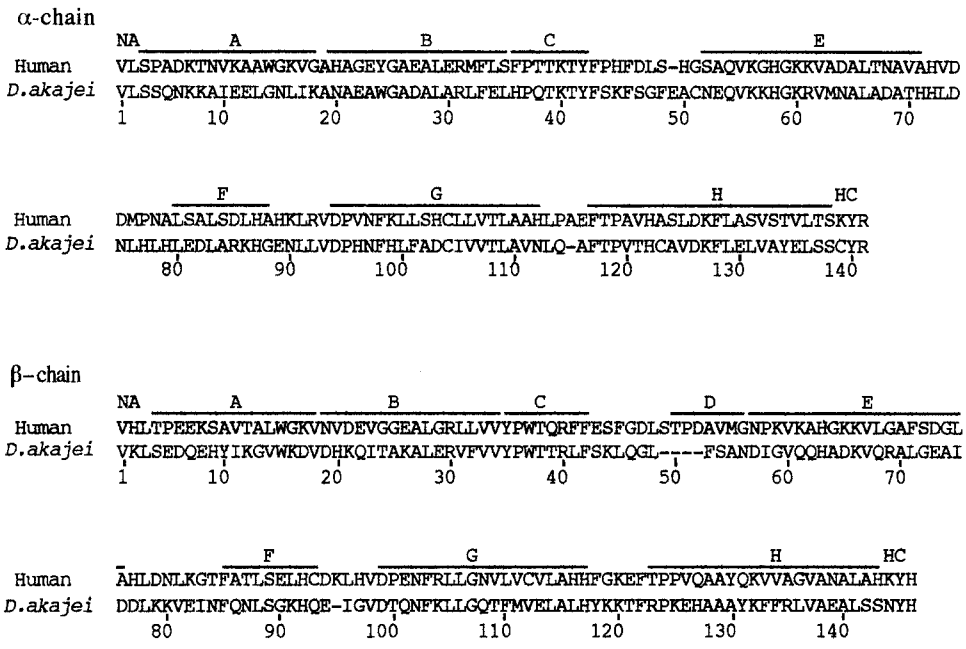

Figure 3
The amino-acid sequences derived from cDNA for α and β subunits of *D. aklajei* Hb are compared with those of human HbA. The residue numbers are those of human HbA.

using *X-PLOR* (Brünger, 1992) in the resolution range 8.0–1.6 Å, during which the *R* factor dropped from 47 to 29%. The restraining parameters used were those of Engh & Huber (1991). Several stages of refinement was carried out using *X-PLOR*; after each round of refinement, $2F_o - F_c$ maps and omit maps in the loop regions and N- and C-termini were calculated and manual adjustment was carried out with the program *FRODO* (Jones, 1978). Coordinates with electron density greater than 3σ in $F_o - F_c$ maps and 1σ in $2F_o - F_c$ maps were designated as water molecules if the locations were reasonable for hydrogen bonding and the temperature factors were not greater than 50 Å^2 (70 Å^2 for the CO form). The initial model for an $\alpha\beta$ dimer of the CO form was constructed from the deoxy form and an analogous procedure was adopted for the refinement. Crystallographic and refinement data are summarized in Table 1.

Coordinates of human HbA (deoxy, 2hhb; CO, 2hco), *P. bernacchii* Hb (deoxy, 1hbh; CO, 1pbx) and trout Hb I (deoxy, 1out; CO, 1ouu) were taken from the Protein Data Bank (Abola *et al.*, 1987).

3. Results and discussion

3.1. Oxygen equilibrium properties

The oxygen equilibrium characteristics are presented in Table 2. *D. akajei* Hb shows a slightly lower oxygen affinity than that of human HbA, with moderate haem–haem interaction, Bohr effect and ATP effect (Imai, 1982). The Bohr effect between pH 6.5 and pH 7.4 without organic phosphate was about 70% that of HbA. ATP reduces the oxygen affinity in neutral and acidic conditions, but the effect is smaller than the 2,3-diphosphoglycerate (DPG) effect of human HbA (Imai, 1982). The oxygen affinity and Bohr effect of Hb from *D. sabina*, another stingray, are similar to *D. akajei* Hb, but this protein shows no ATP effect and the Hill coefficient at neutral pH is lower (Mumm *et al.*, 1978). However, of the 14 N-terminal amino acids of the β subunit, only seven are identical to those of *D. akajei* Hb. Further comparisons are difficult without the complete primary sequence of the protein from *D. sabina*.

3.2. Overview of the structure

It has been concluded from the amino-acid sequence that cartilaginous fish Hbs are also tetrameric $\alpha_2\beta_2$ Hbs (Dickerson & Geis, 1983). Despite the low sequence identity between *D. akajei* Hb and human HbA (about 39%) and the missing D helix in the β subunit of *D. akajei* Hb (see Fig. 3), their overall structures are very similar. In fact, the main-chain atoms of the *D. akajei* Hb tetramer superimpose on those of HbA with an r.m.s. difference of 1.5 Å in the deoxy form and 1.7 Å in the CO form (see Table 6).

Fig. 1 shows the r.m.s. deviations of main-chain atoms by residue between *D. akajei* Hb and human HbA.[1] The large deviations (up to 6 Å) around β50 are the result of the deletion of four residues in *D. akajei* Hb. Other insertions or deletions (one in the β subunit and two in the α subunit) cause deviations of about 2–3.5 Å, which are also seen in other regions. Relatively large changes in the *A* helix, *CD* corner and C-terminal residues are observed in other fish Hbs (Camardella *et al.*, 1992; Mylvaganam *et al.*, 1996) and are attributable to the flexible nature of these regions. The comparatively large deviations between the beginning of the *E* helix and the end of the *F* helix (especially in the β subunit) are peculiar to the stingray Hb. In this region of the β subunit, the r.m.s. deviations vary periodically in both the deoxy and CO forms (Fig. 1*b*). Along the *E* helix, external residues show larger r.m.s. deviations from HbA. These deviations of the *E* and *F* helices are discussed further below.

Fig. 2 shows the r.m.s. deviation of main-chain atoms between $\alpha_1\beta_1$ dimers of the CO and deoxy forms of *D. akajei*

[1] The $\alpha_1\beta_1$ interface (involving mainly the *B*, *G* and *H* helices of the two subunits) is relatively invariant (Baldwin & Chothia, 1979) and has been used as the frame for superpositions of different Hbs. The *BGH* core residues used for the superposition in this paper are the main-chain atoms of *B*5–*B*15, *G*4–*G*18, *H*3–*H*17 for both α and β subunits. The r.m.s. deviations of the superimposed main-chain atoms of *D. akajei* Hb and human HbA are 0.56 and 0.57 Å for the deoxy and CO forms, respectively.

Table 3
Haem geometries of deoxy and CO forms.

Distances are in Å.

	Fe–Nε†	Fe–P_N ‡	Fe–P_C §	P_N–P_C¶
Deoxy human α chain	2.14	0.40	0.55	0.15
Deoxy human β chain	2.03	0.36	0.46	0.10
CO human α chain	2.09	0.00	0.02	0.02
CO human β chain	2.08	−0.02	−0.01	0.01
Deoxy *D. akajei* α chain	2.17	0.31	0.49	0.18
Deoxy *D. akajei* β chain	2.20	0.26	0.40	0.14
CO *D. akajei* α chain	2.17	0.02	0.02	0.00
CO *D. akajei* β chain	2.12	0.01	0.06	0.05

† Fe–Nε, the distance between Fe and Nε of His (F8). ‡ Fe–P_N, the separation of Fe and the mean plane of pyrrole N atoms. § Fe–P_C, the separation of Fe and the mean plane of 20 porphyrin C atoms. ¶ P_N–P_C, doming of porphyrin.

Table 4
The r.m.s. deviations (Å) of the main-chain atoms of the *E* helix, *EF* corner, *F* helix and all these regions in the haem frame (superimposing porphyrins of two Hbs: four pyrroles and four methine C atoms) and in the *BGH* frame of the $\alpha_1\beta_1$ interface of *D. akajei* Hb and human HbA.

	Haem frame		BGH frame	
	Deoxy	CO	Deoxy	CO
α chain				
E helix (*E*4–*E*20)	1.25	0.89	0.70	1.03
EF corner (*EF*1–*EF*8)	0.83	0.82	1.31	0.95
F helix (*F*1–*F*9)	0.54	0.67	0.87	0.82
Total	1.01	0.82	0.92	0.96
β chain				
E helix (*E*3–*E*20)	1.56	0.76	1.93	2.25
EF corner (*EF*1–*EF*8)	1.37	1.28	1.39	1.79
F helix (*F*1–*F*9)	1.15	1.07	0.92	1.86
Total	1.42	0.98	1.60	2.03

Hb in the *BGH* frame (r.m.s. deviation 0.357 Å). Baldwin & Chothia (1979) have performed similar calculations for human HbA. The most significant deviations in Figs. 2(*a*) and 2(*b*) start from the end of the *E* helix, rise to a maximum around the *FG* corner and tail off at the beginning of the *G* helix. HbA shows a similar pattern. Thus, the tertiary structure changes of $\alpha_1\beta_1$ dimers upon CO binding are essentially the same for *D. akajei* Hb and human HbA.

3.3. The primary structure

Fig. 3 shows the primary structures of the α and β chains of *D. akajei* Hb (determined from cDNA sequences) compared with those of human HbA. The α chain, as in human HbA, contains 141 residues, but in the *D. akajei* Hb α chain an extra glutamic residue is present next to α49(CD7) (Ser for human HbA and Phe for *D. akajei* Hb) and one residue is deleted at GH3. The β chain also contains 141 residues, five residues less than the β chain of human HbA; four residues from *CD*8 to *D*3 of HbA and one at *FG*2 are deleted. In the case of single-residue deletions or insertions, two to three successive residues show distinctly different conformations, so deciding the precise position of the mutation is a matter of choice. We selected the second residue of the three as the deleted (or inserted) one. Sometimes deviation between two main chains at the selected site is smaller than those at both of the adjacent sites. In the case of the four-residue deletions in the β subunit, we selected the middle four residues of the six residues found with distinctly different conformations. As a result of this deletion, the *D* helix is missing from the β subunit of *D. akajei* Hb. Three other primary sequences for Hbs of cartilaginous fish, *Heterodontus portusjacksoni* (Nash *et al.*, 1976; Fisher *et al.*, 1977), *Squalus acanthias* (Aschauer *et al.*, 1985) and *Torpedo marmorata* (Huber & Braunitzer, 1989), have been reported. In these Hbs, a single-residue insertion in the *CD* corner and a single-residue deletion in the *GH* corner in the α subunit in addition to a four- or five-residue deletion in the β subunit are present in common. The *D* helix has also been deleted from the β subunit of HbA and reinserted into the α subunit by site-directed mutagenesis. Neither change greatly altered the oxygen equilibrium of the protein (Komiyama *et al.*, 1991). The deletion of β(*FG*2) seems unique to *D. akajei* Hb. The N-termini of the α chain for bony fish Hbs are usually acetylated, but the electron-density map of the *D. akajei* α subunit shows no indication of acetylation. This is consistent with the fact that the N-terminal amino-acid sequence could be readily determined using an automated protein sequencer.

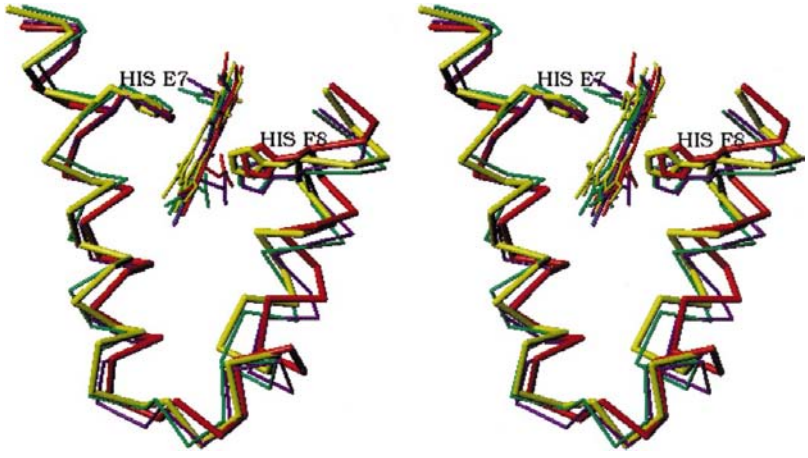

Figure 4
A stereoscopic comparison of β haems and C^{α} traces of the *E* helix, *EF* corner and *F* helix with the side chains of proximal and distal His residues in the *BGH* frame. CO form of *D. akajei* Hb (red, bold), deoxy form of *D. akajei* Hb (blue, thin), CO form of human HbA (yellow, bold), deoxy form of human HbA (green, thin). The structure of the deoxy form of human HbA is superimposed on the structure of *D. akajei* deoxy-Hb. The structure of the CO form of human HbA is superimposed on the structure of the deoxy form of human HbA. The structure of the CO form of *D. akajei* Hb is superimposed on the structure of *D. akajei* deoxy-Hb. CO molecules are not shown.

3.4. Haem-group region

The alteration in haem geometry upon ligation of *D. akajei* Hb, which flattens and moves the Fe atom to an in-plane position, is very similar to

that of HbA (Table 3; Fermi *et al.*, 1984). There are no significant mutations in the haem region that would be expected to alter ligand affinity directly. In *D. akajei* deoxy-Hb there is a water molecule in the α haem pocket, similar to that seen in the α subunit of human deoxy-Hb (Fermi *et al.*, 1984).

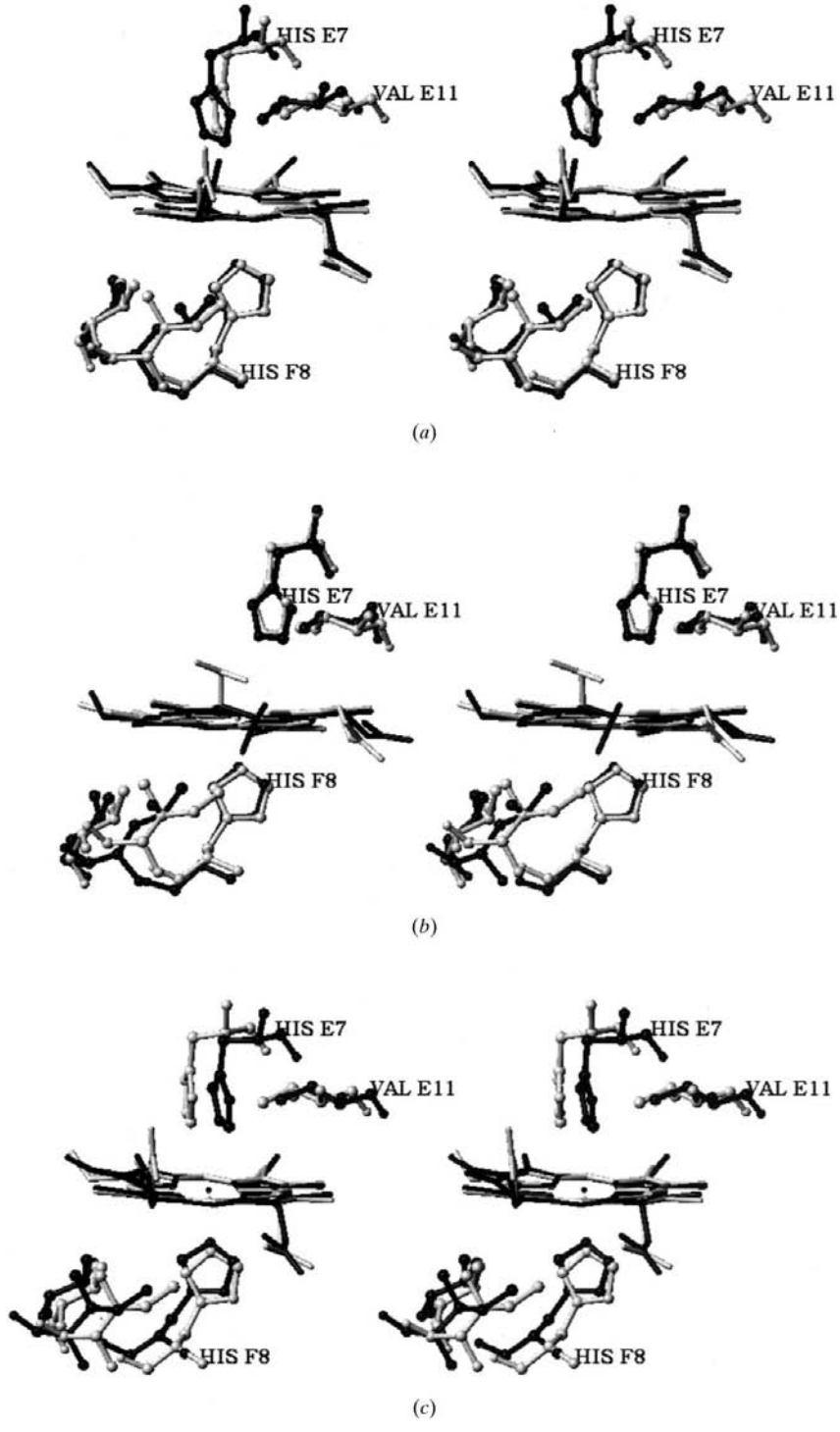

Figure 5
Stereoscopic comparisons for the haems and their environs of the β subunit in the haem frame. (*a*) CO form of *D. akajei* Hb (white) and HbA (black), (*b*) deoxy form of *D. akajei* Hb (white) and HbA (black), (*c*) CO (black) and deoxy (white) forms of *D. akajei* Hb. CO molecules are not shown.

In the *BGH* reference frame, the haems in both the α and β subunits of *D. akajei* Hb move further into haem pocket in the direction from pyrrole *A* to pyrrole *C* ($\sim$0.8 Å for the α subunit and $\sim$1.5 Å for the β subunit). In human HbA, the β-subunit haem rotates $\sim$9° upon CO binding about an axis in the haem plane and perpendicular to the translational movement described above (pyrrole *A* moves to the distal side upon CO binding), whereas in the α subunit there is no such rotation (Baldwin & Chothia, 1979). On the other hand, in *D. akajei* Hb there are similar but smaller rotations of haems in both the α and β subunits. In order to highlight the relation between the displacement of haems and the deviations of the *E* helix, *EF* corner and *F* helix shown in Fig. 1(*b*), we calculated the r.m.s. deviations of these parts in the haem frame (superimposing porphyrins of two Hbs: four pyrroles and four methine C atoms) as well as in the *BGH* frame of the $\alpha_1\beta_1$ interface (Table 4). Most of the r.m.s. deviations between *D. akajei* Hb and HbA become smaller on going from the *BGH* frame to the haem frame, indicating that the relative movement between haems and *E* helix, *EF* corner and *F* helix is smaller than their movement in the whole molecule. A marked reduction takes place in the CO form β subunit.

In order to investigate the reduction in detail, a stereoscopic comparison of the β-subunit region with the side chains of the distal and the proximal His in the *BGH* frame of the $\alpha_1\beta_1$ interface is shown in Fig. 4. Relatively large structural differences between *D. akajei* Hb and HbA are seen around the β haems. On the distal side, the entire *E* helices in both the deoxy and CO forms of *D. akajei* Hb are displaced relative to those of human HbA. In Fig. 1(*b*), it is observed that the external residues are displaced more than the internal residues. Fig. 4 shows that the movement of the *E* helix includes a small rotation about an axis almost parallel to the helix axis, which displaces the external residues more. Close inspection shows that the displacements of side-chain atoms close to the haem are smaller than those of the C^{α} atoms to which they are attached (only the distal and proximal His are shown in Fig. 4). Comparison of displacements on the proximal side of the β haem is complicated by the deletion at the *FG*2 position in *D. akajei* Hb. The movement of the *F* helix towards the *FG* corner and change in haem tilt upon CO ligation appear similar to the changes in HbA (Baldwin &

Chothia, 1979). In the haem frame, these displacements become much smaller. In the carbonmonoxy structures, the positions of the side chains of Val (E11), His (E7) and His (F8) are nearly identical in HbA and the stingray protein (Fig. 5*a*). In the deoxy form, the displacement of the distal Val β(E11) γ2 methyl group between *D. akajei* Hb and human HbA is about 1 Å (Fig. 5*b*), which reduces the movement of Val (E11) upon ligation of CO (Fig. 5*c*). The distances between the ligand O atom and the C atom of the γ2 methyl group of Val (E11) in the deoxy form in the haem frame are 1.6 and 2.6 Å for human HbA and *D. akajei* Hb, respectively. Although the displacement of Val (E11) is much smaller in *D. akajei* Hb, it is still stereochemically important. The smaller movement of Val (E11) seems to correlate with the smaller tilting of the β haem upon CO ligation, as there is more room for the ligand in deoxy *D. akajei* Hb as a result of the deletion of the *D* helix, making the β subunit more α-like.

As suggested by the sequence, the structural changes in the α subunit (Table 4) are smaller than those in the β subunit, although some are still significant. However, no changes are found among the haem-contact side chains that appear to be functionally important. In common with the β subunit, the mutations between HbA and the stingray protein alter the haem environment relatively little. Interestingly, the distal valine Val63 α(E11) moves away about the same distance as that of the β subunit from the ligand-binding site upon CO binding in *D. akajei* Hb, whereas only a small movement was observed in human HbA (Shaanan, 1983). As noted above, this movement in the β subunits is more marked in the human protein.

3.5. $\alpha_1\beta_1$ contact region

Of the 33 residues participating in this contact tabulated by Fermi & Perutz (1981) for deoxy-HbA, only 16 are found unaltered in *D. akajei* Hb. From Fig. 1 it can be seen that these changes have not altered the relative position of the subunits within the $\alpha\beta$ dimer. Pro α119(H2) is an important residue at the $\alpha_1\beta_1$ contact in human HbA; it is highly conserved among vertebrate Hbs and lies close to β55(D6), a methionine in HbA. It is replaced by alanine in Hb from the high-flying bar-headed goose, which has been correlated with a higher oxygen affinity (Zhang *et al.*, 1996). Loss of the β *D* helix greatly alters the contact, as the path of the polypeptide chain is shifted. Gly β29(B11) of HbA is mutated to Glu in *D. akajei* Hb and occupies the space filled by Met β55(D6) in HbA. Although the closest approach of α119(H2) and β29(B11) is about 4.4 Å (compared with a distance of about 3.8 Å between the proline and methionine of HbA) it seems that Glu β29(B11) replaces this contact.

3.6. $\alpha_1\beta_2$ contact region

The $\alpha_1\beta_2$ ($\alpha_2\beta_1$) contact involves mainly the *C* helix, *G* helix and *FG* corner, and is termed the sliding contact, since it undergoes the largest relative movement between deoxy Hb and HbCO. The movement can be approximated as a rigid-body rotation of the $\alpha_2\beta_2$ dimer relative to the $\alpha_1\beta_1$ dimer by 15° about a pivot passing through the α subunits. The contact between the α *FG* corner and β *C* helix is called the flexible joint because it is near the pivot point and is relatively unchanged on ligand binding, while the contact between the β *FG* corner and α *C* helix is called the switch region because it is further away from the pivot point and slides extensively (Baldwin & Chothia, 1979).

In the switch region of deoxy human HbA, Thr41 α1(C6) sits between His97 β2(FG4) and Asp99 β2(G1) but is replaced in the CO form by Thr38 α1(C3). In *D. akajei* Hb, βFG4 is mutated to Gly and αC3 to Gln. Fig. 6(*a*) shows the structural differences in the switch region by superimposing the main-chain atoms in the α1 *C* helix of *D. akajei* deoxy-Hb on those of deoxy-HbA. The displacement of the β2 *FG* corner of *D. akajei* deoxy-Hb from deoxy-HbA is apparent: β*FG*4 and β*G*1 residues of *D. akajei* Hb are displaced about 1.9 Å from those of HbA in the direction from α41 to α38. However, in *D. akajei* deoxy-Hb Thr41 α1(C6) is still between Gly92 β2(FG4) and Asp94 β2(G1). In the CO form, a similar displacement of the β2 *FG* corner is observed, but Gln38 α1(C3) is still between Gly92 β2(FG4) and Asp94 β2(G1). Fig. 6(*b*) shows the β*FG* corner sliding along the

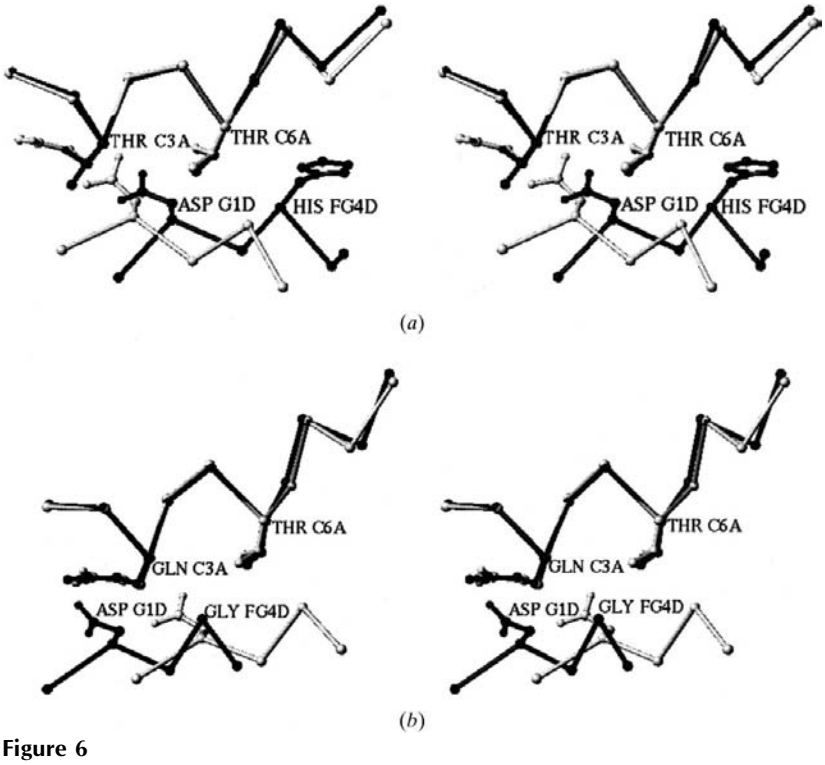

Figure 6
A stereoscopic comparison of the switch region of the $\alpha_1\beta_2$ contact after the superposition of the *C* helix of the α subunit. The letters *A* and *D* in the residue labelling represent α_1 and β_2, respectively. Only the residues of human HbA are presented in (*a*). (*a*) *D. akajei* deoxy-Hb (white) and deoxy-HbA (black). (*b*) *D. akajei* deoxy-Hb (white) and the CO form of *D. akajei* Hb (black).

Table 5
Interatomic distances (Å) between hydrogen-bonded residues in the $\alpha_1\beta_2$ contact of *D. akajei* Hb and human HbA.

Deoxy form.

α_1	β_2	*D. akajei*	Human †
Tyr C7	Asp G1	2.7	2.5
Asp G1	Trp C3	2.9	3.0
Asn G4	AspG1	2.9	2.8

CO form.

α1	β2	*D. akajei*	Human †
Asp G1	Asn G4	3.0	2.8

† The figures were adapted from Tame *et al.* (1996).

αC helix upon CO binding. It is obvious that the essential sliding mechanism in the switch region is maintained. The substitution of Gly for His β(FG4) may have been selected to relieve steric strain with α1(C6) in the deoxy form and α1(C3) in the CO form. The loss of this His may partly explain the smaller Bohr effect. A similar examination of the joint regions of *D. akajei* deoxy-Hb and deoxy-HbA shows smaller differences than in the switch region (the displacements of FG4 and G1 were 0.7 and 0.8 Å, respectively). In deoxy-HbA, Arg α1(FG4) and Arg β2(C6) lie close together but are antiparallel, so the two guanidium groups are held apart. Arg at αFG4 is replaced by Leu in the fish protein without affecting the sliding mechanism.

Of the 31 residues participating in this contact tabulated by Fermi & Perutz (1981) for deoxy-HbA, ten are found to be altered in *D. akajei* Hb (Fig. 3). Most of the human Hb variants with the same single amino-acid substitution per dimer as that of *D. akajei* Hb show some degree of functional abnormality. We have mentioned two of them above, which appear to be the most important. However, the substitutions of Gly for His at βFG4 and of Leu for Arg do not appear to have a large effect on protein function. The key intersubunit hydrogen bonds previously identified as important in maintaining the allosteric equilibrium are all preserved in *D. akajei* Hb (Table 5; Dickerson & Geis, 1983; Ishimori *et al.*, 1992).

3.7. Bohr effect

The chloride-independent part of the Bohr effect of HbA largely arises from the β-subunit C-terminal residue His146β(HC3), which forms salt bridges with Asp94β(FG1) in the same subunit through the imidazole group and with Lys40α(C5) across the $\alpha_1\beta_2$ contact through its carboxyl group (Perutz *et al.*, 1998). In *D. akajei* Hb, β(HC3) and α(C5) are occupied by the same residues but Asp (FG1) is replaced by Glu, in common with other fish Hbs. Fig. 7 shows the $F_o - F_c$ electron-density map for *D. akajei* deoxy-Hb, in which Asn139 β(HC1), Tyr140 β(HC2), His141 β(HC3) and Gln89 β(F9) were omitted for the calculation of the electron density. The imidazole of the C-terminal His is not oriented towards Glu90 β(FG1), but instead forms a hydrogen bond with the β-carbonyl group of Asn139 β(HC1). The C-terminal carboxyl group forms hydrogen bonds with the ε amino group of Lys40 α(C5) (not shown) and simultaneously with the γ-amide group of Gln89 β(F9) in *D. akajei* Hb. The model indicates two reasons for this conformational difference. Firstly, Cys 93β(F9) in HbA is replaced by Gln in *D. akajei* Hb, which obstructs the salt bridge between the imidazole group of His β(HC3) and Asp β(FG1). Secondly, the deletion of Lys95 β(FG2) of HbA in *D. akajei* Hb moves Glu90 β(FG1) further away from the imidazole group of His 141β(HC3) compared with HbA. In the CO form, the imidazole of His141 β(HC3) hydrogen bonds with the γ carbonyl group of Gln89 β(F9). This is confirmed by the $F_o - F_c$ omit map omitting the C-terminal three residues of the β chain. The electron density for the omit map of the CO form is comparatively weak, indicating that the hydrogen bond may be weaker than that in the deoxy form. Thus, it is possible to attribute some of the Bohr effect to the hydrogen bond between the imidazole group of His 141β(HC3) and Asn 139β(HC1) in the deoxy form. Hb from *T. marmorata*, another ray, shows no Bohr effect. In the β chain of this Hb, both F9 and HC1 are occupied by Gln, FG1 is Lys and HC3 is His (Huber & Braunitzer, 1989). Although a similar arrangement for the β C-terminal region of *D. akajei* Hb is possible, the changes at HC1 and FG1 appear to suppress the chloride-independent Bohr effect. Similarly, Hb from the shark *Selachii acanthias* shows a Bohr effect less than half (~40%) that of human HbA in the absence of chloride (Weber *et al.*, 1983). In the β subunit of this Hb, F9 is Tyr, FG1 is Glu, HC1 is Gly and HC3 is His. F9 Tyr would obstruct salt-bridge formation between FG1 Glu and HC3 His, and HC1 Gly cannot form a hydrogen bond with HC3. The sequences and Bohr effects seen in these fish

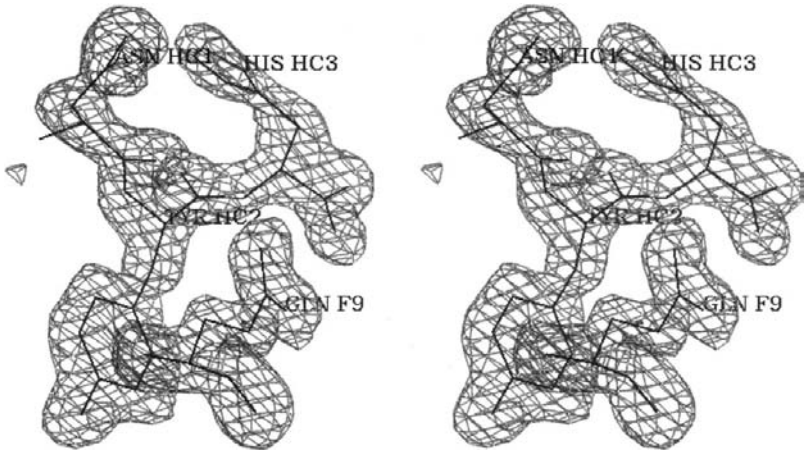

Figure 7
A stereoscopic $F_o - F_c$ electron-density map of *D. akajei* deoxy-Hb at 2σ in the C-terminal region of the β subunit. Four residues [Asn139 β(HC1), Tyr140 β(HC2), His141 β(HC3) and Gln89 β(F9)] are omitted for the calculation of the electron density.

Table 6
The pairwise r.m.s. deviations (Å) of main-chain atoms in the helical portions of Hbs.

Helical portions used for the superposition are *A*1–16, *B*1–16, *C*1–7, *E*1–20, *F*1–9, *G*1–19 and *H*1–21 for the α subunit; *A*1–15, *B*1–16, *C*1–7, *E*1–20, *F*1–9, *G*1–19 and *H*1–18 for the β subunit. Upper right: CO form. Lower left: deoxy form.

	Human	*P. bernacchii*	Trout Hb I	*D. akaeji*
Human		1.2	1.2	1.7
P. bernacchii	1.2		0.9	1.7
Trout Hb I	1.1	0.9		1.6
D. akajei	1.5	1.5	1.4	

Hbs are therefore consistent with the structure of *D. akajei* Hb.

In the α C-terminal region, the structure of *D. akajei* deoxy-Hb and human HbA are very similar. Slightly larger changes appear between the CO forms, but none of them appear to be functionally significant. One conspicuous feature of *D. akajei* Hb is Tyr α134 (Thr in HbA) situated near the molecular dyad axis and parallel with the symmetry-related equivalent tyrosine from the other α subunit. These two phenol groups form an aromatic stacking interaction, lying about 3.5 Å apart. In the CO form, together with two C-terminal Args, these two Tyrs effectively plug the central cavity.

3.8. Organic phosphate-binding sites

ATP lowers the oxygen affinity of *D. akajei* Hb (Table 2). A model for the binding site of ATP in bony fish Hbs has been proposed (Perutz & Brunori, 1982; Perutz, 1983). In this model, the same residues [Lys β(EF6), His β(H21), His β(NA2) and β N-terminal α-amino group] used for human HbA to bind 2,3-diphosphoglycerate (DPG) participate in the binding of ATP. In bony fish Hb, Glu or Asp is substituted for His at NA2 and Arg for His at H21, but the former can be modelled to accept a hydrogen bond from adenine and the latter to participate in the binding of phosphate. In *D. akajei* Hb, however, βEF6 is Glu, βH21 is Ser and βNA2 is Lys. Thus the organic phosphate-binding site corresponding to that of human deoxy-HbA cannot bind ATP.

We have searched for other polyanion-binding sites in *D. akajei* deoxy-Hb along the molecular dyad and found in the central cavity, just inside the DPG-binding site of deoxy HbA, a pair of positive charges on the ε amino group of Lys 99β(G6) and the guanidinium group of Arg 130β(H13) (separated by about 3.6 Å between Nε and Cζ). The distance between the symmetry-related Lys Nε atoms is about 11.4 Å and the shortest distance between the Arg side chains is about 8.9 Å. This space is squeezed upon CO binding as is the DPG-binding site. The closest distance between the *H* helices is the distance between the C$^{\alpha}$ atoms of Glu134 β(H17): 13.3 Å in *D. akajei* deoxy-Hb and 8.5 Å in the CO form. Although we have not attempted to model ATP into the structure, this site is a possible candidate for an ATP-binding site of *D. akajei* Hb.

A novel β_1–β_2 interaction was identified for the CO form of *D. akajei* Hb. The side chain of Arg130 β(H13) is hydrogen bonded to the main-chain carbonyl groups of Ser137(H20) and Tyr140(HC) of the other β subunit. Although the side-chain atoms have higher *B* factors than average, this structure was confirmed in the omit map, where the side-chain atoms were excluded from the structure-factor calculation.

3.9. Comparison of the structures of cartilaginous fish, bony fish and human HbA

The pairwise r.m.s. deviations of main-chain atoms in the helical portions of human HbA, *P. bernacchii* Hb, trout Hb I and *D. akajei* Hb in both the deoxy and CO forms are presented in Table 6. Naturally, the r.m.s. deviations between the two bony fish Hbs are small, because they are genealogically closely related. The sequence identity between them is about 56%. *D. akajei* Hb differs more than the bony fish Hbs from human HbA. This agrees with our observations that structural differences in various regions of *D. akajei* Hb are apparently larger than those described for *P. bernachii* Hb (Camardella *et al.*, 1992; Ito *et al.*, 1995) and for trout Hb I (Tame *et al.*, 1996). On the other hand, the r.m.s. distances of the two bony fish Hbs are similar to that of human HbA when referred to *D. akajei* Hb. Very similar relations are found for the superposition of the CO-form tetramers. Thus, the r.m.s. distances in Table 6 are consistent with both the genealogical separation of the animals and the sequence similarity of their Hbs. We have not analyzed the structure differences among vertebrate Hbs further, because we think that further structure determinations of Hbs which diverged in the early stage of vertebrate evolution are necessary.

4. Conclusions

Although there are structural differences in various parts of *D. akajei* Hb and human HbA, the two Hbs are functionally similar and the basic nature of the quaternary structure change upon CO binding are the same. On the other hand, the mechanism of the Bohr effect and organic phosphate effect seem to be different. These facts show marked contrast to the results obtained for functionally abnormal mutant human Hbs. Some of them show very high oxygen affinity by only a single amino-acid substitution per $\alpha\beta$ dimer, yet in most cases the crystal structures are unchanged except around the mutated position. Thus, we are led to conclude that there are many functional compensations in the amino-acid substitutions which reach up to 60% of the total sequence between *D. akajei* Hb and human HbA, and that the evolution of the function of Hb is a result of many compensating mutations.

The authors thank Dr J. Tame of the University of York, England, for critical reading of the manuscript and for helpful advice. They also thank Dr M. Kusunoki of the Research Center for Protein Research, Institute of Protein Research, Osaka University for help with the data collection and the subsequent analysis. They are grateful to Drs Y. Kawasaki and

T. Suzuki of the Department of Biology, Faculty of Science, Kochi University for help with N-terminal sequencing and cloning. Data collection at the Photon Factory was performed under the approval of the Photon Factory Advisory Committee (Proposal No. 95G061). HM is a member of the TARA project of Tsukuba University. This work was partly supported by a Grant-in-Aid from Scientific Research on Priority Area (protein three-dimensional structure) from the Ministry of Education, Science and Culture of Japan.

References

Abola, F. C., Bernstein, F. C., Bryant, S. H., Koetzle, T. F. & Weng, J. (1987). *Crystallographic Databases – Information Content, Software Systems, Scientific Applications*, pp. 107–132. Bonn, Cambridge, Chester: IUCr.

Aschauer, H., Weber, R. E. & Braunitzer, G. (1985). *Biol. Chem. Hoppe-Seyler*, **366**, 589–599.

Baldwin, J. & Chothia, C. (1979). *J. Mol. Biol.* **129**, 175–220.

Bashfold, D., Chothia, C. & Lesk, A. M. (1987). *J. Mol. Biol.* **196**, 199–216.

Brünger, A. T. (1992). *X-PLOR Version* 3.1. *A System for X-ray Crystallography and NMR*. New Haven, CT: Yale University Press.

Camardella, L., Caruso, C., D'Avino, R., di Prisco, G., Rutigliano, B., Tamburrini, M., Fermi, G. & Perutz, M. F. (1992). *J. Mol. Biol.* **224**, 449–460.

Dickerson, R. E. & Geis, I. (1983). *Haemoglobin: Structure, Function, Evolution and Pathology*. Menlo Park, California: Benjamin/Cummings.

Engh, R. A & Huber, R. (1991). *Acta Cryst.* A**47**, 392–400.

Fermi, G. & Perutz, M. F. (1981). *Haemoglobin and Myoglobin, Atlas of Molecular Structures in Biology*, edited by D. C. Phillips & F. M. Richards. Oxford: Clarendon Press.

Fermi, G., Perutz, M. F., Shannan, B. & Fourme, R. (1984). *J. Mol. Biol.* **175**, 159–174.

Fisher, W. K., Nash, A. R. & Thompson, E. O. P. (1977). *Aust. J. Biol. Sci.* **30**, 487–506.

Huber, F. & Braunitzer, G. (1989). *Biol. Chem. Hoppe-Seyler*, **370**, 831–838.

Imai, K. (1982). *Allosteric Effects in Haemoglobin.* Cambridge University Press.

Imai, K., Morimoto, H., Kotani, M., Watari, H., Hirata, W. & Kuroda, M. (1970). *Biochim. Biophys. Acta*, **200**, 189–196.

Ishimori, K., Imai, K., Miyazaki, G., Kitagawa, T., Wada, Y., Morimoto, H. & Morishima, I. (1992). *Biochemistry*, **31**, 3256–3264.

Ito, N., Komiyama, N. H. & Fermi, G. (1995). *J. Mol. Biol.* **250**, 648–658.

Jones, T. A. (1978). *J. Appl. Cryst.* **11**, 268–272.

Komiyama, N. H., Shih, T.-B. D., Looker, D., Tame, J. & Nagai, K. (1991). *Nature (London)*, **352**, 349–351.

Lesk, A. M. & Chothia, C. (1980). *J. Mol. Biol.* **136**, 225–270.

Lynch, R. E., Lee, G. R. & Cartwright, G. E. (1976). *J. Biol. Chem.* **251**, 10515–10519.

Mumm, D. P., Atha, D. H. & Riggs, A. (1978). *Comput. Biochem. Physiol. B*, **60**, 189–193.

Mylvaganam, S., Bonaventura, C., Bonaventura, J. & Getzoff, E. (1996). *Nature Struct. Biol.* **3**, 275–283.

Nash, A. R, Fisher, W. & Thompson, E. O. P. (1976). *Aust. J. Biol. Sci.* **30**, 487–506.

Otwinowski, Z. & Minor, W. (1997). *Methods Enzymol.* **276**, 307–326.

Perutz, M. F. (1968). *J. Cryst. Growth*, **2**, 54–56.

Perutz, M. F. (1983). *Mol. Biol. Evol.* **1**, 1–28.

Perutz, M. F. & Brunori, M. (1982). *Nature (London)*, **299**, 421–426.

Perutz, M. F., Wilkinson, A. J., Paoli, M. & Dodson, G. (1998). *Annu. Rev. Biophys. Biomol. Struct.* **27**, 1–34.

Rossmann, M. G. & Blow, D. M. (1962). *Acta Cryst.* **15,** 24–31.

Sakabe, N. (1983). *J. Appl. Cryst.* **16**, 542–547.

Shaanan, B. (1983). *J. Mol. Biol.* **171**, 31–59.

Suzuki, T., Arita, T. & Kawasaki, Y. (1996). *Zool. Sci.* **12**, 453–455.

Suzuki, T. & Nishikawa, T. (1996). *J. Protein Chem.* **15**, 389–394.

Tame, J. R. H., Wilson, J. C. & Weber, R. E. (1996). *J. Mol. Biol.* **259**, 749–760.

Weber, R. E., Wells, R. M. G. & Rossetti, J. E. (1983). *J. Exp. Biol.* **103**, 109–120.

Winterbourn, C. C., McGrath, B. M. & Carrell, R. W. (1976). *Biochem. J.* **155**, 493–502.

Zhang, J., Hua. Z., Tame, J. R. H., Lu, G., Zhang, R. & Gu, X. (1996). *J. Mol. Biol.* **255**, 484–493.